SENSORY ANALYSIS FOR A NEW DYNAMIC BALANCING SYSTEM BASED ON MAGNETIC INTERACTION

Cristinel ILIE[1], Daniel COMEAGA[2], Octavian DONTU[3]

The paper presents an analysis of the sensory subsystem as a part of a novel dynamic balancing system based on magnetic interaction, without using active magnetic bearings. Solutions to improve the measuring linearity are proposed and discussed. The described technical solution is based on a patent of the principal author.

Keywords: dynamic balancing, measuring principle, measuring nonlinearity

1. Introduction

In this article it is proposed a new dynamic balancing system, based on a patent of the principal author, which uses a new principle, where the motion transmission and bearings for the balancing part are made using magnetic interaction, without mechanical contact. These are not active magnetic bearings; the lifting and motion transmission using magnetic field are achieved with permanent magnets [1].

The usual approach used for correction of a rotor unbalance is to mount it on the elastic bearings of a balancing machine and put it into a uniform rotating motion; the reactions due to mechanical unbalance will produce forced vibrations of bearings, which will be measured using a suitable sensory subassembly (for classical solutions, with accelerometers or electrodinamichal transducers) and resulting an electrical signal; this electrical signal will provide information regarding the unbalance [2].

The motion transmission from the driving motor to the balanced rotor is always accompanied by undesired vibrations that affect the main vibration due to the rotor unbalance.

The errors may be caused by a variety of reasons, including eccentricity and axial run-out in drive element, misalignment of bearings, lack of concentricity of journal and bearing surfaces, errors due to stripping and reassembling, etc.

[1] Eng, PhD student, National Institute for Research and Development in Electrical Engineering, ICPE-CA, Romania, e-mail: cristinel.ilie@icpe-ca.ro
[2] Assoc. prof., Dept. of Mechatronics and Precision Mechanics, University POLITEHNICA of Bucharest, Romania, e-mail: comeaga_daniel@yahoo.com
[3] Prof., Dept. of Mechatronics and Precision Mechanics, University POLITEHNICA of Bucharest, România, e-mail: octavdontu@yahoo.com

Considering these undesired problems, a lot of work was performed before solve them by using new technical approach, in order to reduce damaging influences of external factors. These approaches have tried to improve the functioning of existing machines. As an example, an improved solution, developed by T. Dragomir and I. Silea [3], and also by S. Zhou, J. Shi [4] was an active balance of the rotors using active magnetic bearings. Although with many technical advantages, the active bearings have a few drawbacks, regarding the bearing loading, the price and the complexity of the active control system [5].

Much simpler and cheaper is the solutions presented in this article where the bearings and the couplings have been achieved with permanent magnets.

In this case, the sensory subassembly uses a displacement transducer.

2. Technical solution

The basically sketch of the chosen technical solution is presented in Fig. 1

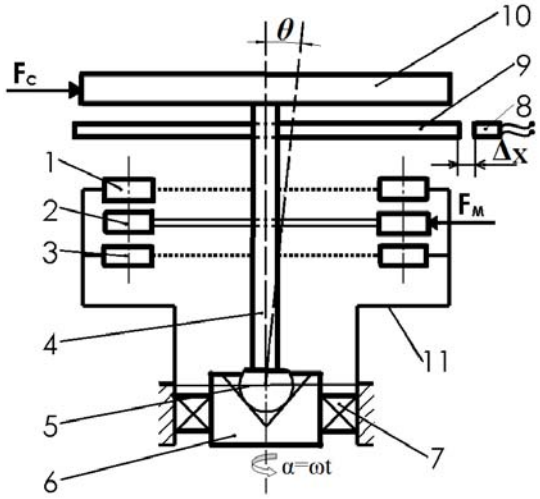

Fig. 1 The basically sketch of the dynamic balancing system

The main part of the design is a special structure with permanent magnets in radial arrangement on the surface of three concentric disks. Each disk has the same number of permanent magnets in a hetero-polar arrangement on the circumference. The magnets will be set one in front of the other, so that axial gaps occur. The middle disk (2) is fixed on the interior spindle (the driven spindle) (4). This middle disk is placed between the static disks (1) and (3), which are fixed on the driving spindle (11). All three disks are building an axial magnetic coupling. By fixing together the external disks (1) and (3), the axial attraction forces between the three disks are balanced.

An important advantage of the structure is self-centering by using magnetic interaction for the disks 1-2-3, which are equipped with permanent magnets.

This mentioned advantage leads to the fact that this kind of coupling acts also as a radial lifting system (radial bearing) without mechanical contact at the exit end of the internal spindle. The stiffness (the variation of the radial force versus the forced radial displacement) has relative high values. For this reason the recommended permanent magnets must have a stiff characteristic of the magnetization, as those of rare earth magnets [6]. NdFeB permanent magnets have been used. The permanent magnets have a cylindrical shape.

The sensory subassembly consist of a displacement transducer (8) and a transducer disk (9).

3. Working principle

The balancing part (10) is concentric mounted on the spindle (4), like in Fig. 1. The external spindle (11) is put into a uniform rotating motion, using mostly a transmission belt (not shown in figure 1).

Due to the existing magnetic coupling, the disks (1) and (3) bring into motion the disk (2), by magnetically interaction and also the tested part (10) and the transducer disk (9).

The chosen option removes the active magnetic bearing-system and replaces it with a simple spherical bearing-system, composed by the spherical part (5) and the lining (6), which provides the relative position of the disk (2) against the disks (1) and (3)

The central spindle (4) executes together with the balancing part (10) and with the transducer disk (9) a precession motion. It can be approximated as first step in modeling, that they execute a precession motion with a constant angular velocity, the nutation angle is constant and without oscillation movement relative to the mobile shaft axis.

Due to the dynamic equilibrium of the forces and moments from magnetic coupling with the forces and moments produced by centrifugal force unbalances, it result result a linear relationship between the value of dynamic unbalance of the balanced part and the precession angle, θ [7].

It has been demonstrated both by analytical calculation, assuming a plane-parallel displacement of the disc (9), and by numerical simulation method, that between the magnetic interaction radial force F_M (which is in opposition with the centrifugal force F_c) and radial displacement Δ_X of the transducer disk (9) there is a linear proportionality [8].

By analysis of the force-system it can be seen that the unbalance of the part is proportional to its displacement angle θ, for low values of the angle.

Disk (9), fixed on spindle (4), will have a radial displacement, whose component in the perpendicular plane to the rotation axis is Δx, will be measured by the sensory subassembly consisting of a transducer disk (9) and a displacement transducer (8). After numerical processing of the data, one can determine the level of the unbalance, depending on the Δx displacement.

Further, it will be studies several measurement principles for radial displacement of the balanced part Δ_X, depending on the transducer type.

4. Sensory system modeling

The dependence between the angle θ and the radial displacement x, which is measured with a displacement sensor (8) is analyzed.

In order to do this, one uses the notations from Fig. 2:

- R=swivel radius of the disc (9) measured from the center of rotation of ball bearing;
- r= transducer disk (9) radius;
- θ = angular displacement of the shaft (4).

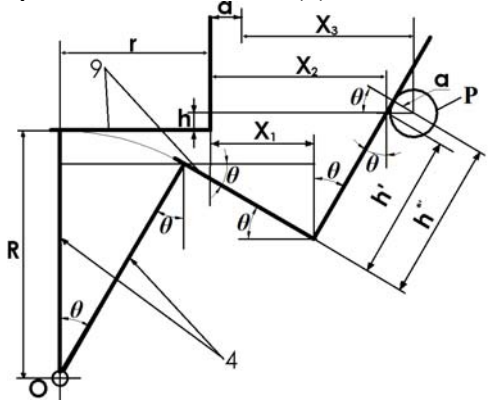

Fig. 2 Equivalent model to determine the relation x=f(θ)

In three cases the dependence between the displacement x versus the θ angle is analyzed that differ by the type of the transducer measuring principle. The displacements for the three cases are noted with X_1, X_2 and X_3.

Case 1. The X_1 displacement is determined in case of using a displacement transducer, which is not influenced by tilting or disc (9) thickness (for example an inductive transducer).

This is the case when the diameter of the transducer is much higher than the height of the mobile disk transducer (9) (Fig.3a). If the diameter of the transducer is much lower than the height of the mobile disk transducer, one measures the displacement X_2, analyzed in the case 2 (Fig. 3b).

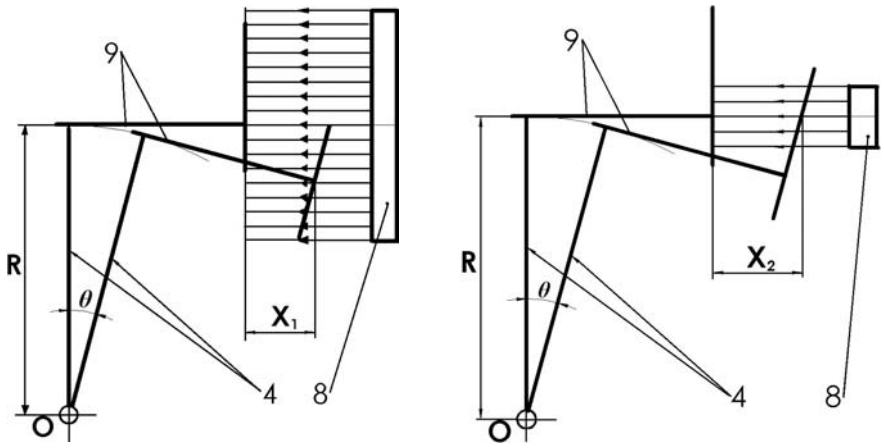

Fig. 3 Equivalent model to measuring the displacement using a inductive displacement transducer (a) and using a laser displacement transducer (b)

After projection of the geometric elements on X-axis, it follows:

$$x_{11}^{\theta} = r\cos\theta + R\sin\theta - r = R\sin\theta - r(1-\cos\theta) \tag{1}$$

For large values of the angle θ, the equation (1) shows a nonlinearity of the measurement principle.

For very small values of the angle θ, sinθ = θ and cosθ = 1, and equation (1) becomes:

$$x_{1}^{\theta} = R\theta - r(1-1) \cong R\theta \tag{2}$$

From equation (2) a linear dependence between the transducer signal versus the angle θ results.

Case 2. The X_2 displacement is determined in case of using a proximity transducer with a very thin „beam" as a laser one, whose incident measuring beam is - in the equilibrium position, at the distance *h* from disc(9) lower surface and at the distance *h'* when the shaft (4) is tilted with the angle θ. In this case, the measurement is influenced by tilting and disc (9) thickness.

After projection of the geometric elements on X and Y axes, it follows:

$$x_{21}^{\theta} = (R+h)tg\theta + r\left[-1+\frac{1}{\cos\theta}\right] \tag{3}$$

For large values of the angle θ, the equation (3) shows a higher nonlinearity of the measurement principle than in the previous case.

For very small values of the angle θ, sinθ = θ and cosθ = 1 and the equation (3) becomes:

$$x_{2}^{\theta} = (R+h)\theta \tag{4}$$

From equation (4) a linear dependence between the transducer signal versus the θ angle results.

Case 3. The X_3 displacement is determined in the case of using a mechanical proximity transducer, with a spherical testing spike (P) with radius *a*, whose incident measure point is - in the equilibrium position, at the distance *h* from disc (9) lower surface and at the distance $h^{*\prime}$ when the shaft (4) is tilted by the angle θ. In this case also, the measurement is influenced by the tilting and the thickness of the disk (9) (Fig. 2).

After projection of the geometric elements on X and Y axes, it follows:

$$x_{31}^{\theta} = (R+h)tg\theta + (a+r)\left(\frac{1}{\cos\theta} - 1\right) \tag{5}$$

For large values of the angle θ, the equation (5) shows a high nonlinearity of the measurement principle.

For very small values of the angle θ, sinθ = θ and cosθ = 1, equation (5) becomes:

$$x_3^{\theta} \cong (R+h)\theta \tag{6}$$

From equation (6) a linear dependence between the transducer signal versus the θ angle results.

Observations

According to the basic sketch of the calculation model, shown in Fig. 3, the proximity transducer measures the displacement of the disk (9) when it has an angular clockwise displacement (+ θ) to the vertical position of equilibrium (it gets closer to the transducer). If calculations are performed to measure the disc (9) displacement on the x-axis, when it is at an angular symmetrical position to the vertical position of equilibrium, (-θ), it is found that this displacement is different from the initial position measured value. For case 1, this is shown in Fig. 4.

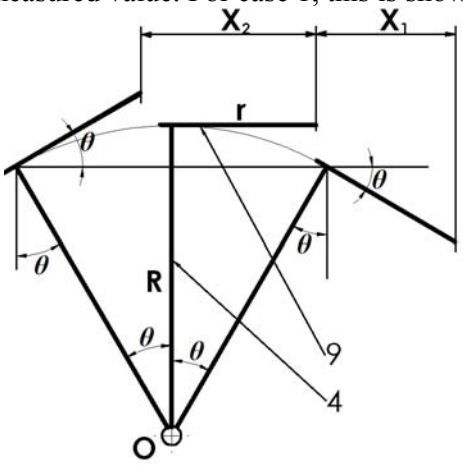

Fig. 4. X displacement versus (-θ)angle

Case 1. After projection of the geometric elements on X-axis, it results the equation (7), obtained from the equation (1), where the angle θ has been replaced with the angle (-θ).

$$x_{11}^{-\theta} = -[R\sin\theta + r(1-\cos\theta)] \tag{7}$$

Case 2. For a negative displacement it is obtained the relation (8), is obtained from equation (3), where the angle θ has been replaced with the angle (-θ).

$$x_{21}^{-\theta} = -\left\{(R+h)tg\theta + r\left[1-\frac{1}{\cos\theta}\right]\right\} \tag{8}$$

Case 3. For a negative displacement it is obtained the relation (9), is obtained from equation (5), where the angle θ has been replaced with the angle (-θ).

$$x_{31}^{-\theta} = -\left\{(R+h)tg\theta + (a+r)\left(1-\frac{1}{\cos\theta}\right)\right\} \tag{9}$$

For all three cases, it can be seen that the value of the measured signal for a negative displacement angle (-θ) is different from the signal measured for a positive angle θ, antipodal measured.

This is a source of errors that will have a negative impact on the accuracy of the unbalance measurement.

However, carefully analyzing the pairs of equations (1-7), (3-8) and (5-9), it is observed that errors introduced by disc (9) diameter, can be removed, if the equations for x^{θ} and $x^{-\theta}$ are added, term by term. The influence of the disk radius, and possibly of the touch ball diameter are removed. In this case, two transducers placed diametrically opposed are used.

It result:

Case 1 $$x_{12} = x_{11}^{\theta} - x_{11}^{-\theta} = 2R\sin\theta \tag{10}$$

Case 2 $$x_{22} = x_{21}^{\theta} - x_{21}^{-\theta} = 2(R+h)tg\theta \tag{11}$$

Case 3 $$x_{32} = x_{31}^{\theta} - x_{31}^{-\theta} = 2(R+h)tg\theta \tag{12}$$

It is seen from equations (10), (11) and (12) that the useful signal value will be twice as large and some of the terms that introduce measurement nonlinearity will be removed; this will allow to obtain an increased sensitivity for the unbalance system determination.

Another conclusion, that can be used to reduce the errors, results from an analysis of the equations (1), (3) and (5), and consists in minimizing the *r* radius.

The effect is similar to the use of two transducers. The influence of the disk (9) radius is removed but not remove the influence of the ball touch radius is not cancelled. In this case the sensitivity is twice lower compared to the case

shown above. The advantage is however a simpler construction (a single-transducer, a single data acquisition channel, etc.)

If $r \approx 0$, it results:

Case 1 $$x_{13} = R\sin\theta \tag{13}$$

Case 2 $$x_{23} = (R+h)tg\theta \tag{14}$$

Case 3 $$x_{33} = (R+h)tg\theta - a\left(1-\frac{1}{\cos\theta}\right) \tag{15}$$

Basically, this is obtained by mounting the proximity transducer closer to the rotation axis of the shaft (4).

The nonlinearity errors for case 1, when the measurement is done with a single inductive transducer Δx_{11}, or using two transducers in opposite positions Δx_{12}, or by neglecting the *r* radius of the disk (9) Δx_{13}, are:

$$\Delta x_{11} = R\sin\theta - r(1-\cos\theta) - R\theta \tag{16}$$

$$\Delta x_{12} = 2R\sin\theta - 2R\theta \tag{17}$$

$$\Delta x_{13} = R\sin\theta - R\theta \tag{18}$$

Similar equations are obtained for case 2, using a laser transducer:

$$\Delta x_{21} = (R+h)tg\theta - r\left[1-\frac{1}{\cos\theta}\right] - R\theta \tag{19}$$

$$\Delta x_{22} = 2(R+h)tg\theta - 2R\theta \tag{20}$$

$$\Delta x_{23} = (R+h)tg\theta - R\theta \tag{21}$$

And for case 3, using a mechanical contact transducer:

$$\Delta x_{31} = (R+h)tg\theta - (a+r)\left(1-\frac{1}{\cos\theta}\right) - R\theta \tag{22}$$

$$\Delta x_{32} = 2(R+h)tg\theta - 2R\theta \tag{23}$$

$$\Delta x_{33} = (R+h)tg\theta - a\left(1-\frac{1}{\cos\theta}\right) - R\theta \tag{24}$$

In Fig. 5, the equations giving the nonlinearity errors of the signal, in case 1 are plotted.

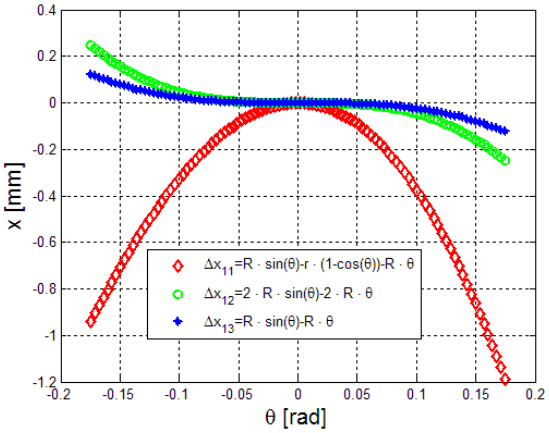

Fig. 5 The nonlinearity signal for case 1

In Fig. 6 the equations giving the nonlinearity errors of the signal in case 2 are plotted.

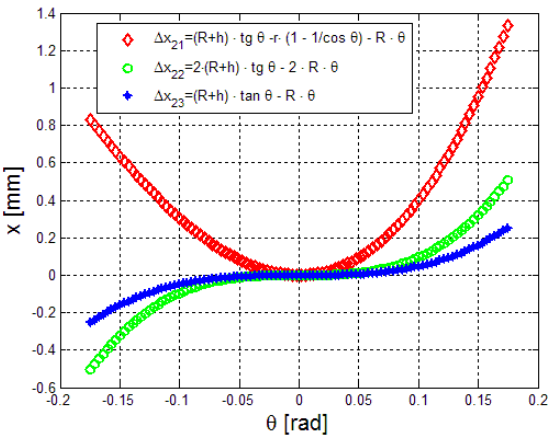

Fig. 6 The nonlinearity signal for case 2

Design data for the charts, following the notations from Fig. 2, is:

- Swivel radius of the disc (9) from the center of rotation of ball bearing R=141 mm
- Disk radius (9), r= 60mm
- Distance between the direction of incident laser beam and lower disc surface (9), h=3mm
- Radius of the spherical testing spike(P), a=2mm

In Fig. 7 the equations giving the nonlinearity errors of the signal are plotted in case 3.

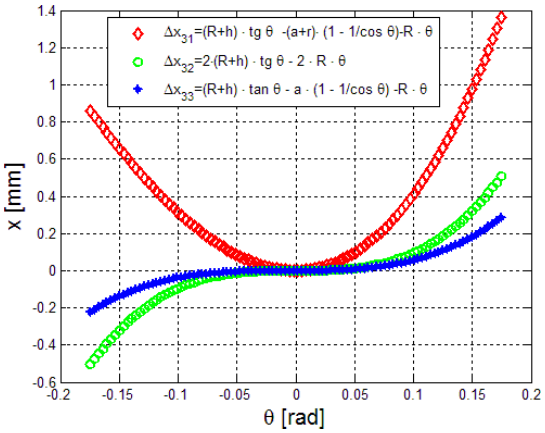

Fig. 7 The nonlinearity signal for case 3

The results shown in the Figs. 5, 6 and 7, have been achieved using the software MathLab2009.

The field with the best linearity results from the analysis of the numerical data provided by the MathLab program.

Thus, for a relative error, $\Delta x_{ij}/x_{ij}$, lower than 1‰, it results:

For case 1- when a inductive displacement transducer is used

$$\theta_{11} = \pm 2{,}92^0 \qquad \theta_{12} = \pm 8{,}79^0 \qquad \theta_{13} = \pm 8{,}79^0 \tag{25}$$

For case 2- when a laser displacement transducer is used

$$\theta_{21} = \pm 2{,}92^0 \qquad \theta_{22} = \pm 6{,}97^0 \qquad \theta_{23} = \pm 6{,}97^0 \tag{26}$$

For case 3- when a mechanical contact displacement transducer is used

$$\theta_{31} = \pm 2{,}92^0 \qquad \theta_{32} = \pm 9{,}19^0 \qquad \theta_{33} = \pm 7{,}73^0 \tag{27}$$

where $\theta_{11}...\theta_{33}$ have been determined in accordance with the signal values $x_{11}..x_{33}$ and with the nonlinearity errors of the signal $\Delta x_{11}...\Delta x_{33}$.

In practice a supplementary error appear due to the tilting of the disk. The measurements shown in Fig. 2 should be computed again considering not only the beveling of the disk having the rotation axis in the plane created by the transducer axis and the axis of the shaft (11) but also the movement of the disk (9) out of this plane. This additional movement creates other nonlinear terms in the previous equations, difficult to remove even by signal processing. The proposed solution was to use two opposite transducer on the same diameter of the stator (the shaft 11) whose signals are measured continuously and saved in the memory only when the values are maximum and respectively minimum. In this situation, the axes of shafts 11, 4 and the axes of transducers are in the same plane, as it is represented in Fig. 2. The saved values are processed according with the algorithm described above.

5. Conclusion

In this paper, nine possibilities to measure the useful signal were presented.

Three of them use an inductive displacement transducer, three of them use a laser displacement transducer, and three use a mechanical displacement transducer.

For each of these three cases, the useful signal measurement can be done in three different ways: 1) using a single transducer which measures the movement of a transducer disk, that moves together with the balanced part; 2) using two transducers placed diametrically opposed, each of them measures the movement of a transducer disk, that moves together with the balanced part; 3) using a single transducer which measures the movement of the balanced part, by mounting the transducer closer to the rotation axis of the part (the useful signal is not influenced by the transducers disk radius).

From the analysis of the numerical values showing in (25-27) it follows that the best situation is to use a sensory subsystem that used two transducers placed diametrically opposed. In these situations, the tilting angles θ are the largest (θ_{12}, θ_{22}, θ_{32}).

It can be noticed that good values are obtained also in the case of using a mechanical contact displacement transducer, in accordance with θ_{23} from (27). However, it is not recommended to use this type of transducer due to shortcomings of the transducers with mechanical contact.

From the point of view of practical design of the dynamic balancing system, the best type of transducers is an inductive displacement transducer, that allows the largest inclination for the mobile shaft, θ_{12} (and therefore the highest useful signal).

Also, good results are obtained when a single transducer which is mounted closer to the rotation axis of the parts, (θ_{13}, θ_{23}, θ_{33}) is used.

We mention that this situation could be applied rarely, due to the construction configuration of the system.

As it has been shown above, the new balancing system is feasible - there is linearity between unbalance of the rotor and the signal of the proximity transducer.

R E F E R E N C E S

[1] *W. Kappel, G. Mihaiescu, C. Ilie, D. Lipcinski, I. Vasile,* Dispozitiv de echilibrare dinamica cu cuplaj mahnetic, Brevet 123090/30.09.2010.

[2] *Derek Norfield,* Practical Balancing of Rotating Machinery, ELSEVIER Lth. ISBN 10:1-85-617465-4, 2005.

[3] *T. L. Dragomir, I. Silea,* Control system for the magnetic bearings of a balancing machine, Journal of Electrical Engineering, Vol 3/2003, Universitatea Politehnica Timisoara.
[4] *S. Zhou, J. Shi*, Active Balancing and Vibration Control of Rotating Machinerj: A Survey, The Shock and Vibration Digest, Vol. 33, No. 4, July 2001, 361-371.
[5] *G. Schweizer,* Active magnetic bearings-chances and limitations, Intrenational Centre for Magnetic Bearings, ETH Zurich, www.mcgs.ch/web.
[6] *H. Gavrilă, H. Chiriac, P. Ciureanu, V. Ioniță, A.Yalon*; Magnetism tehnic şi aplicat*,* Editura Academiei Române, Bucureşti, 2000.
[7] *Cristinel Ilie, Daniel Comeaga, Octavian Dontu,* Modeling and Testing of a New Dynamic Balancing System Based on Magnetic Interaction, Conference AVMS 2013, ACOUSTICS AND VIBRATION OF MECHANICAL STRUCTURES, May 23-24, 2013, Timisoara.
[8] *Cristinel Ilie, Daniel Comeaga, Adrian Nedelcu,* Modeling and Simulation of a New Dynamic Balancing System Based on Magnetic Interaction, The 8th International Symposium on ADVANCED TOPICS IN ELECTRICAL ENGINEERING, ATEE 2013, May 23-25, 2013, Bucuresti.